

# Improved phase sensitivity of an SU(1,1) interferometer based on the internal single-path local squeezing operation

Qingqian Kang<sup>1,2</sup>, Zekun Zhao<sup>1</sup>, Teng Zhao<sup>1</sup>, Cunjin Liu<sup>1</sup>, and Liyun Hu<sup>1,3\*</sup>

<sup>1</sup>Center for Quantum Science and Technology, Jiangxi Normal University, Nanchang 330022, China

<sup>2</sup>Department of Physics, College of Science and Technology,  
Jiangxi Normal University, Nanchang 330022, China

<sup>3</sup>Institute for Military-Civilian Integration of Jiangxi Province, Nanchang 330200, China

Compared to passive interferometers, SU(1,1) interferometers exhibit superior phase sensitivity due to the incorporation of nonlinear elements that enhance their ability to detect phase shifts. However, the precision of these interferometers is significantly affected by photon losses, especially internal losses, which can limit the overall measurement accuracy. Addressing these issues is essential to fully realize the advantages of SU(1,1) interferometers in practical applications. Among the known resources of quantum metrology, one of the most practical and efficient is squeezing. We propose a theoretical scheme to improve the precision of phase measurement using homodyne detection by implementing the single-path local squeezing operation (LSO) inside the SU(1,1) interferometer, with the coherent state and the vacuum state as the input states. We not only analyze the effects of the single-path LSO scheme on the phase sensitivity and the quantum Fisher information (QFI) under both ideal and photon-loss cases but also compare the effects of different squeezing parameters  $r$  on the system performance. Our findings reveal that the internal single-path LSO scheme can enhance the phase sensitivity and the QFI, effectively improving the robustness of the SU(1,1) interferometer against internal and external photon losses. Additionally, a larger squeezing parameter  $r$  leads to a better performance of the interferometer.

PACS: 03.67.-a, 05.30.-d, 42.50.Dv, 03.65.Wj

## I. INTRODUCTION

Quantum precision measurement technology is a method that utilizes quantum resources and effects to achieve measurement accuracy beyond traditional methods. It integrates multidisciplinary knowledge such as atomic physics, physical optics, electronic technology, and control technology, leveraging principles of quantum mechanics, particularly the superposition and entanglement properties of quantum states, to accomplish highly accurate measurements. This technology has a wide range of applications [1–7], including high-precision optical frequency standards and time-frequency transfer, quantum gyroscopes, atomic gravimeters, and other quantum navigation technologies, as well as quantum radar, trace atom tracking, and weak magnetic field detection in quantum sensitive detection technologies. These technologies have significant application potential in fields such as inertial navigation, next-generation time referencing, stealth target identification, global terrain mapping, medical testing [8], and fundamental physics research [9].

Phase estimation is a crucial method for precision measurement, offering a way to estimate many physical quantities that cannot be directly measured through conventional methods. Consequently, extensive research and significant advancements have been made in the field of optical interference measurement. To satisfy the demand for high precision, various optical interferometers have been proposed and developed. One of the most

practical interferometers is the Mach-Zehnder interferometer (MZI), whose phase sensitivity is limited by the standard quantum-noise limit (SQL)  $\Delta\phi_{SQL} = 1/\sqrt{N}$  ( $N$  is the average number of photons within the interferometer), together with solely classical resources as the input of the MZI [10]. In recent decades, various schemes have been proposed to enhance the phase sensitivity of the traditional MZI [11, 12]. It has been shown that using quantum states as input can enable the traditional MZI to surpass the SQL. For instance, NOON states [13], twin Fock states [14], squeezed states [15, 16], and photon-catalyzed squeezed vacuum states [17] can achieve or even exceed the Heisenberg limit (HL)  $\Delta\phi_{HL} = 1/N$  [18].

In 1986, Yurke *et al.* [19] introduced the SU(1,1) interferometer, which replaced traditional beam splitters (BSs) with optical parametric amplifiers (OPAs). In the SU(1,1) interferometer consisting of two OPAs, the first OPA serves the dual purpose of generating entangled resources and suppressing amplified noise. The subsequent use of the second OPA enhances the signal, providing a viable pathway to achieving higher precision in phase estimation [20]. By utilizing entangled photon states, the SU(1,1) interferometer can surpass the SQL, enabling greater precision. This technique has revolutionized phase estimation, becoming a vital tool in quantum precision measurements. In 2011, Jing *et al.* [21] successfully implemented this interferometer experimentally. For instance, Hudelist *et al.* demonstrated that the gain effect of OPAs enables the SU(1,1) interferometer exhibiting higher sensitivity compared to traditional linear interferometers [22]. This has led to a growing interest in exploring the SU(1,1) interferometer [23, 24].

\* hlyun@jxnu.edu.cn

Apart from the standard form, various configurations of SU(1,1) interferometer have also been proposed [25–33].

As previously mentioned, although SU(1,1) interferometer is highly valuable for precision measurement [34, 35], the precision is still affected by dissipation, particularly photon losses inside the interferometer [36, 37]. Consequently, to further enhance precision, non-Gaussian operations can effectively mitigate internal dissipation. Most theoretical [38–41] and experimental [42–44] studies have indicated that non-Gaussian operations are effectively enhancing the nonclassicality and entanglement degrees of quantum states, thereby enhancing their potential in quantum information processing [45].

It is evident that the use of non-Gaussian operations indeed improves the estimation performance of optical interferometers, but this comes at a high implementation cost. To address the aforementioned problem, Gaussian operations such as the LSO [46–48] and the local displacement operation (LDO) [49, 50] have emerged as promising strategies. In Ref. [50], Ye *et al.* investigated phase sensitivity and QFI based on homodyne detection in the presence and absence of photon losses through displacement-assisted SU(1,1) [DSU(1,1)], involving two LDOs within the SU(1,1) interferometer. In this DSU(1,1) interferometer, the introduced LDOs improved phase sensitivity and QFI even under realistic conditions. It is important to emphasize that the LSO is crucial not only in quantum metrology [46] but also in quantum key distribution [47] and entanglement distillation [48]. These applications demonstrate the versatility and significance of the LSO in advancing various quantum technologies, highlighting its role in enhancing precision measurements and ensuring secure communication protocols. In Ref. [46], J. Sahota and D. F. V. James proposed an innovative quantum-enhanced phase estimation scheme that applies the LSO to both paths of the MZI. Their work illustrates the potential for the LSO scheme to enhance the performance of interferometric devices, paving the way for advancements in quantum metrology and measurement techniques.

Recent advances in the experimental realization of squeezing operations have opened new avenues for enhancing the precision of optical phase measurements [51–54]. Thus, can the single-path LSO scheme implemented inside the SU(1,1) interferometer similarly enhance the phase sensitivity and the QFI? Can this approach enhance the robustness of the interferometer against internal and external photon losses? If the single-path LSO scheme brings improvements, it would be a better choice from the perspective of quantum resources.

In this paper, we propose a theoretical scheme to improve the precision of phase measurement using homodyne detection by implementing the single-path LSO scheme inside the SU(1,1) interferometer, with the coherent state and the vacuum state as the input states. We also perform a comparative analysis about the effects

of internal and external photon losses on interferometer performance. This paper is arranged as follows. Sec. II outlines the theoretical model of the SU(1,1) interferometer based on the internal single-path LSO scheme. Sec. III delves into phase sensitivity, encompassing both ideal and photon-loss cases. Sec. IV centers on the QFI. Finally, Sec. V provides a summary.

## II. MODEL

This section first describes the standard SU(1,1) interferometer, as shown in Fig. 1(a). The SU(1,1) interferometer, which usually consists of two OPAs and a linear phase shifter, is one of the most commonly used interferometers in quantum metrology studies. The first OPA is characterized by a two-mode squeezing operator  $U_{S_1}(\xi_1) = \exp(\xi_1^* ab - \xi_1 a^\dagger b^\dagger)$ , where  $a$  ( $b$ ) and  $a^\dagger$  ( $b^\dagger$ ) represent the photon annihilation and creation operators, respectively. The squeezing parameter  $\xi_1$  can be expressed as  $\xi_1 = g_1 e^{i\theta_1}$ , where  $g_1$  represents the gain factor and  $\theta_1$  represents the phase shift. This parameter plays a critical role in shaping the interference pattern and determining the system's phase sensitivity. After the first OPA, mode  $a$  undergoes a phase shift process  $U_\phi = \exp[-i\phi(a^\dagger a)]$ , while mode  $b$  remains unchanged. Subsequently, the two beams are coupled in the second OPA with the operator  $U_{S_2}(\xi_2) = \exp(\xi_2^* ab - \xi_2 a^\dagger b^\dagger)$ , where  $\xi_2 = g_2 e^{i\theta_2}$  with  $\theta_2 - \theta_1 = \pi$ . In this paper, we set the parameters  $g_1 = g_2 = g$ ,  $\theta_1 = 0$ , and  $\theta_2 = \pi$ . We use the coherent state  $|\alpha\rangle_a$  and the vacuum state  $|0\rangle_b$  as input states, and homodyne detection is applied to the mode  $a$  of the output.

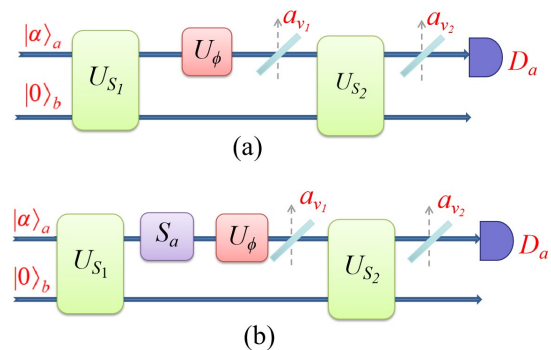


FIG. 1. Schematic diagram of the SU(1,1) interferometer. (a) The standard SU(1,1) interferometer and (b) the SU(1,1) interferometer with the single-path LSO scheme. The two input ports are a coherent state  $|\alpha\rangle_a$  and a vacuum state  $|0\rangle_b$ .  $a_{v_1}$  and  $a_{v_2}$  are vacuum modes.  $U_{S_1}$  and  $U_{S_2}$  are the OPAs, and  $U_\phi$  is the phase shifter.  $S_a$  is the single-path LSO operator and  $D_a$  is the homodyne detector.

The SU(1,1) interferometer is generally susceptible to photon losses, particularly in the case of internal losses. To simulate internal and external photon losses, the use of fictitious BSs is proposed, as depicted in Fig. 1(a). The

operators of these fictitious BSs can be represented as  $U_{B_1}$  and  $U_{B_2}$ , with  $U_{B_1} = \exp[\theta_{T_1}(a^\dagger a_{v_1} - a a_{v_1}^\dagger)]$  and  $U_{B_2} = \exp[\theta_{T_2}(a^\dagger a_{v_2} - a a_{v_2}^\dagger)]$ , where  $a_{v_1}$  and  $a_{v_2}$  represent vacuum modes. Here,  $T_k$  ( $k = 1, 2$ ) denotes the transmissivity of the fictitious BSs, associated with  $\theta_{T_k}$  through  $T_k = \cos^2 \theta_{T_k} \in [0, 1]$ . The value of transmittance equal to 1 ( $T_k = 1$ ) corresponds to the ideal case without photon losses [55]. In an expanded space, the expression for the output state of the standard SU(1,1) interferometer can be represented as the following pure state:

$$|\Psi_{out}^0\rangle = U_{B_2} U_{S_2} U_{B_1} U_\phi U_{S_1} |\psi_{in}\rangle, \quad (1)$$

where  $|\psi_{in}\rangle = |\alpha\rangle_a |0\rangle_b |0\rangle_{a_{v_1}} |0\rangle_{a_{v_2}}$ .

To mitigate the impact of photon losses, we introduce a Gaussian operation inside the SU(1,1) interferometer, called the single-path LSO scheme, as illustrated in Fig. 1(b). Recent advancements in the experimental realization of squeezing operations has significantly contributed to the field of quantum metrology, particularly in enhancing the sensitivity of interferometers beyond the SQL. For instance, Purdy *et al.* [51] experimentally demonstrated strong and continuous optomechanical squeezing of  $1.7 \pm 0.2$  dB below the shot-noise level by exploiting the quantum interaction between laser light and a membrane mechanical resonator in an optical cavity. Meanwhile, Ono *et al.* [52] explored optical spin-squeezing, revealing a quantum advantage of 1.58 over the shot-noise limit for five-photon events, suggesting enhanced performance for quantum metrology applications, despite not achieving sub-shot-noise precision due to experimental imperfections. Furthermore, Zuo *et al.* [53] proposed and experimentally demonstrated a compact quantum interferometer that achieves a sensitivity improvement of  $4.86 \pm 0.24$  dB beyond the SQL by using squeezed states generated within the MZI for phase sensing, resulting in a minimum detectable phase smaller than that of all present interferometers under the same phase-sensing intensity. In 2023, Kalinin *et al.* [54] reported the first experimental demonstration of phase sensitivity enhancement in an interferometer using Kerr squeezing, addressing the challenge of the cumbersome tilting of the squeezed ellipse in phase space. The experimental realization of squeezing operations has advanced significantly, enabling the development of highly sensitive and robust interferometric schemes that surpass classical limits. These advancements hold promise for a wide range of applications, including gravitational wave detection, quantum communication, and precision sensing.

In our scheme, we utilize simple and easy-to-prepare input states ( $|\alpha\rangle_a \otimes |0\rangle_b$ ), and an experimentally feasible homodyne detection. The operator of the single-path LSO inside the SU(1,1) interferometer on mode  $a$  can be written as:

$$S_a = \exp\left[\frac{1}{2}(r e^{-i\pi} a^2 - r e^{i\pi} a^{\dagger 2})\right]. \quad (2)$$

In this case of the single-path LSO scheme applied inside the SU(1,1) interferometer, the output state can be written as the following pure state:

$$|\Psi_{out}^1\rangle = U_{B_2} U_{S_2} U_{B_1} U_\phi S_a U_{S_1} |\psi_{in}\rangle. \quad (3)$$

### III. PHASE SENSITIVITY

Quantum metrology utilizes quantum resources to achieve precise phase measurements [56, 57]. The primary objective is to attain highly sensitive measurements of unknown phases. Phase sensitivity is a crucial parameter because improving it can reduce the uncertainty in phase measurements, thereby enhancing the accuracy of the measurements [58]. Selecting an appropriate detection method to extract the phase information is the crucial final step in the phase estimation process. This step is essential for ensuring the accuracy and reliability of measurement results. Common detection methods include homodyne detection [59, 60], parity detection [17, 61], and intensity detection [62], each offering unique trade-offs among sensitivity, complexity, and practical application. It is important to note that the phase sensitivity of different detection schemes can vary depending on the input state and the design of the interferometer [63]. Homodyne detection is feasible with current experimental techniques [64], and its theoretical calculations are relatively straightforward. Therefore, we opt to use homodyne detection at output port  $a$  to estimate phase sensitivity.

In homodyne detection, the measured variable is one of the two orthogonal components of mode  $a$ , given by  $X = (a + a^\dagger)/\sqrt{2}$ . Based on the error-propagation equation [19], the phase sensitivity can be expressed as

$$\Delta\phi = \frac{\sqrt{\langle\Delta^2 X\rangle}}{|\partial\langle X\rangle/\partial\phi|} = \frac{\sqrt{\langle X^2\rangle - \langle X\rangle^2}}{|\partial\langle X\rangle/\partial\phi|}. \quad (4)$$

Based on Eqs. (3) and (4), the phase sensitivity for the LSO scheme can be theoretically determined. Detailed calculation steps for the phase sensitivity  $\Delta\phi$  of the single-path LSO scheme are provided in Appendix A.

#### A. Ideal case

Initially, we consider the ideal case,  $T_k = 1$  (where  $k = 1, 2$ ), representing the case without photon losses. The phase sensitivity  $\Delta\phi$  is plotted as a function of  $\phi$  for various squeezing parameters  $r$  in Fig. 2. It is shown that: (i) The phase sensitivity improves initially and then decreases as the phase  $\phi$  increases, with the optimal sensitivity deviating from  $\phi = 0$ . (ii) The implementation of the single-path LSO inside the SU(1,1) interferometer significantly enhances the phase sensitivity  $\Delta\phi$ . This enhancement becomes especially pronounced with higher

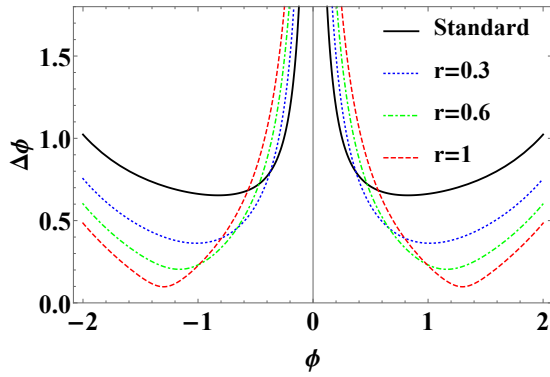


FIG. 2. The phase sensitivity of single-path LSO based on the homodyne detection as a function of  $\phi$  with  $\alpha = 1$  and  $g = 1$ . The black solid line represents the standard SU(1,1) interferometer, while the blue dotted line, green dot-dash line, and red dashed line correspond to squeezing parameters of  $r = 0.3$ ,  $r = 0.6$  and  $r = 1$ , respectively.

squeezing parameters. (iii) As the value of  $r$  increases, the optimal phase sensitivity moves away from  $\phi = 0$ .

Fig. 3 illustrates that the optimal phase sensitivity (minimizing  $\Delta\phi$ ) is plotted against the gain factor  $g$  for different squeezing parameters. The plot confirms that the single-path LSO scheme enhances the phase sensitivity  $\Delta\phi$ . The improvement effect changes little with increasing  $g$ . And, the larger the squeezing parameter  $r$ , the better the phase sensitivity  $\Delta\phi$ .

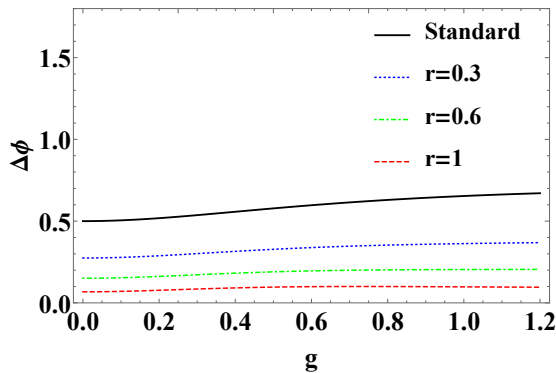


FIG. 3. The phase sensitivity as a function of  $g$ , with  $\alpha = 1$ .

Similarly, we analyze the optimal phase sensitivity (minimizing  $\Delta\phi$ ) as a function of the coherent amplitude  $\alpha$ , as depicted in Fig. 4. The phase sensitivity improves with the coherent amplitude  $\alpha$ , attributed to the increase in the average photon number with  $\alpha$ , then enhancing intramode correlations [65] and quantum entanglement between the two modes. Furthermore, the enhancement effect diminishes as the coherent amplitude  $\alpha$  increases. Again, the larger the squeezing parameter  $r$ , the better the phase sensitivity  $\Delta\phi$ .

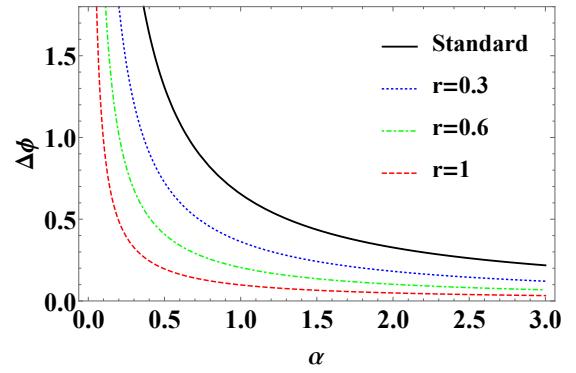


FIG. 4. The phase sensitivity as a function of  $\alpha$ , with  $g = 1$ .

### B. Photon-loss case

The SU(1,1) interferometer plays a critical role in achieving high-precision measurements, but the measurement accuracy is highly sensitive to photon losses. Here, we focus on internal and external photon losses, corresponding to  $T_k \in (0, 1)$ . The optimal phase sensitivity (minimizing  $\Delta\phi$ ), depicted as a function of transmittance  $T_k$  in Fig. 5 for fixed  $g$ ,  $\alpha$ , and  $\phi$ , improves as anticipated with higher transmittance  $T_k$ . Lower transmittance corresponds to increased losses, weakening the performance of phase estimation. Both internal and external photon losses degrade phase sensitivity. Notably, throughout the entire range of  $T_k$ , internal losses have a more significant impact on the system's phase sensitivity. This is primarily because the second OPA amplifies both the signal and the internal noise. The improved effects of phase sensitivity are also clearly observed with an increase in the squeezing parameter  $r$ . In contrast, the phase sensitivity of the single-path LSO scheme is less affected, indicating that the Gaussian operations can mitigate the impact of internal or external photon losses and enhance the interferometer's robustness against losses.

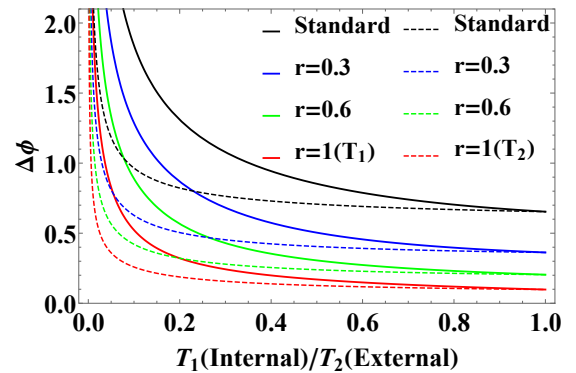


FIG. 5. The phase sensitivity as a function of transmittance  $T_k$ , with  $g = 1$  and  $\alpha = 1$ . The solid lines correspond to internal losses, while the dashed lines correspond to external losses.

### C. Comparison with SQL and HL

Additionally, we compare the phase sensitivity with the SQL and HL in this section. The SQL and HL are defined as  $\Delta\phi_{SQL} = 1/\sqrt{N}$  and  $\Delta\phi_{HL} = 1/N$ , respectively. Here  $N$  represents the total average photon number inside the interferometer before the second OPA for the ideal case [10, 66].  $N$  can be calculated as:

$$\begin{aligned} N &= \langle \psi_{in} | U_{S_1}^\dagger S_a^\dagger (a^\dagger a + b^\dagger b) S_a U_{S_1} | \psi_{in} \rangle \\ &= Q_{1,1,0,0} + Q_{0,0,1,1}, \end{aligned} \quad (5)$$

where the expression of  $Q_{x_1, y_1, x_2, y_2}$  is given in Appendix A.

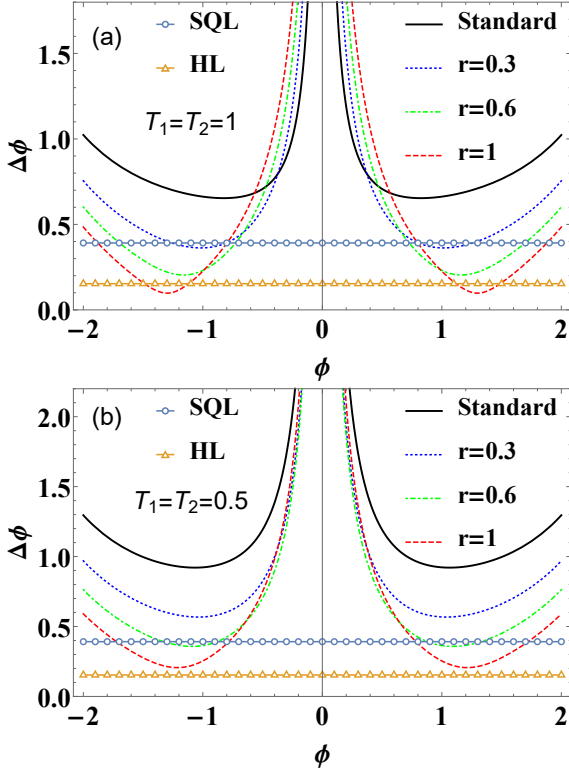


FIG. 6. Comparison of phase sensitivity with the SQL and the HL for fixed  $g = 1$  and  $\alpha = 1$ . The blue circle is the SQL and the yellow triangle is the HL. (a)  $T_1 = T_2 = 1$  and (b)  $T_1 = T_2 = 0.5$ .

For fixed  $\alpha$  and  $g$ , we plot the phase sensitivity  $\Delta\phi$  as a function of  $\phi$  for a comparison with the SQL and the HL of the standard SU(1,1) interferometer in Fig. 6. Our findings demonstrate that: (i) In the ideal case, the phase sensitivity of the standard interferometer (without LSO) cannot surpass the SQL and the HL. However, with the single-path LSO scheme, it can surpass the SQL even when the squeezing parameter  $r$  is relatively small ( $r = 0.3$ ). Moreover, as  $r$  increases, the sensitivity of the LSO scheme can surpass the HL. (ii) In the presence of significant photon losses, the single-path LSO scheme still demonstrates a capability to surpass the SQL when

the squeezing parameter  $r$  is large. As  $r$  increases, the single-path LSO scheme approaches the HL. This indicates that the single-path LSO scheme exhibits strong robustness against photon losses, effectively addressing the challenges posed by photon losses in practical applications.

## IV. THE QUANTUM FISHER INFORMATION

In our previous discussions, we investigated how the single-path LSO scheme affects phase sensitivity and the relationship between various relevant parameters and phase sensitivity through homodyne detection. It is important to note that the phase sensitivity is influenced by the specific measurement method employed. This leads us to the critical question: how can we attain the highest phase sensitivity in an interferometer that is unaffected by the choice of measurement method? In this section, we will turn our attention to the QFI, which indicates the maximum amount of information that can be extracted from the interferometer system, irrespective of the measurement technique used. We will analyze the QFI under both ideal and realistic conditions.

### A. Ideal case

For a pure state system, the QFI can be derived by [67]

$$F = 4 \left[ \langle \Psi' | \Psi' \rangle - |\langle \Psi' | \Psi \rangle|^2 \right], \quad (6)$$

where  $|\Psi\rangle$  is the quantum state after phase shift and before the second OPA, and  $|\Psi'\rangle = \partial |\Psi\rangle / \partial \phi$ . Then the QFI can be reformed as [67]:

$$F = 4 \langle \Delta^2 n_a \rangle, \quad (7)$$

where  $\langle \Delta^2 n_a \rangle = \langle \Psi | (a^\dagger a)^2 | \Psi \rangle - (\langle \Psi | a^\dagger a | \Psi \rangle)^2$ .

In the ideal case, the quantum state is given by  $|\Psi\rangle = U_\phi S_a U_{S_1} |\alpha\rangle_a |0\rangle_b$ . Thus, the QFI is derived as:

$$F = 4(Q_{2,2,0,0} + Q_{1,1,0,0}) - 4(Q_{1,1,0,0})^2, \quad (8)$$

where the expression for  $Q_{x_1, y_1, x_2, y_2}$  is given in Appendix A. It is possible to explore the connection between the QFI and the related parameters using Eq. (8).

Fig. 7 illustrates the QFI as a function of  $g$  ( $\alpha$ ) for a specific  $\alpha$  ( $g$ ). It is evident that a higher value of  $g$  ( $\alpha$ ) corresponds to a greater QFI. The larger the squeezing parameter  $r$ , the greater the QFI. Moreover, we observe that the improvement in QFI due to Gaussian operation increases with the increase of the value  $g$  ( $\alpha$ ).

The minimum value of phase sensitivity achievable for all measurement schemes is known as quantum Cramér-Rao bound (QCRB) as defined by [68]:

$$\Delta\phi_{QCRB} = \frac{1}{\sqrt{vF}}, \quad (9)$$

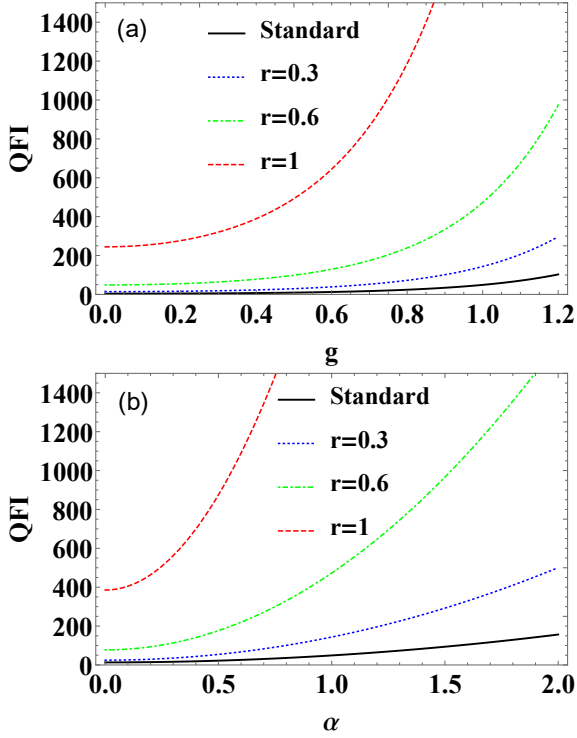


FIG. 7. (a) The QFI as a function of  $g$ , with  $\alpha = 1$ . (b) The QFI as a function of  $\alpha$ , with  $g = 1$ .

where  $v$  represents the number of measurements. For simplicity, we set  $v = 1$ . The QCRB [68, 69], denoted as  $\Delta\phi_{QCRB}$ , establishes the ultimate limit for a set of probabilities derived from measurements on a quantum system. It serves as an estimator implemented asymptotically via maximum likelihood estimation and provides a measurement-independent phase sensitivity. To evaluate the optimality of the phase sensitivity achieved by the SU(1,1) interferometer with the single-path LSO scheme, we analyze the sensitivity  $\Delta\phi_{QCRB}$  derived from the QFI in Fig. 8. It illustrates the variation of  $\Delta\phi_{QCRB}$  as a function of  $g$  ( $\alpha$ ) for a specific  $\alpha$  ( $g$ ). It is shown that  $\Delta\phi_{QCRB}$  improves with increasing  $g$  and  $\alpha$ . Similarly, the larger the squeezing parameter  $r$ , the better the  $\Delta\phi_{QCRB}$ . Furthermore, the improvement in  $\Delta\phi_{QCRB}$  is more obvious for small gain factor  $g$  [refer to Fig. 8(a)] and small coherent amplitude  $\alpha$  [refer to Fig. 8(b)].

### B. Photon losses case

In this subsection, we extend our analysis to cover the QFI in the presence of photon losses. Specifically, we examine homodyne detection on mode  $a$ , which is susceptible to photon losses. Consequently, our attention is directed toward the QFI of the system with photon losses on mode  $a$ , as depicted in Fig. 9. Here, we should emphasize that the Fisher information is obtained using the state preceding the second OPA, i.e., the second OPA is

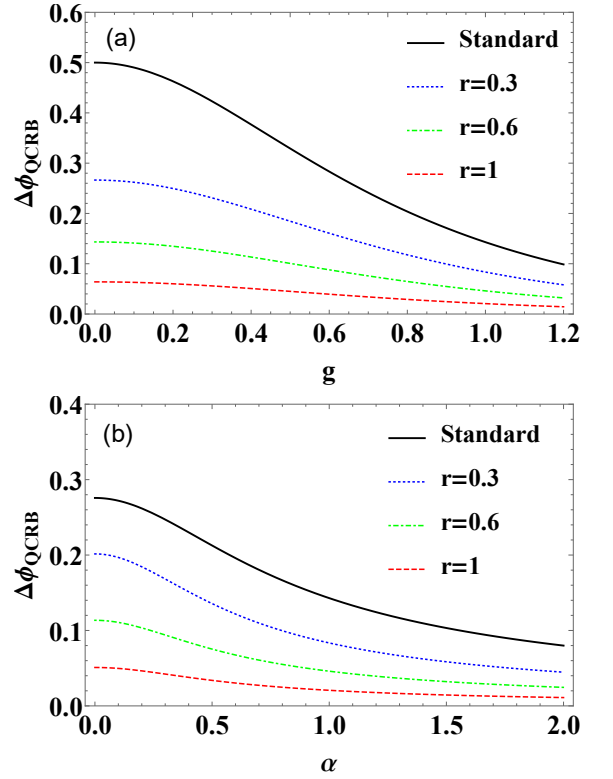


FIG. 8. (a) The  $\Delta\phi_{QCRB}$  as a function of  $g$ , with  $\alpha = 1$ . (b) The  $\Delta\phi_{QCRB}$  as a function of  $\alpha$ , with  $g = 1$ .

not essential. For realistic quantum systems, Escher *et al.* [67] propose a method for calculating the QFI. This method can be briefly summarized as follows.

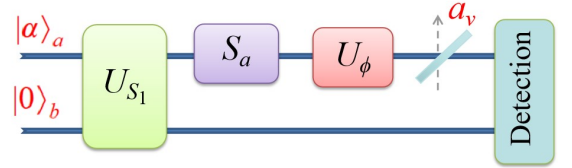


FIG. 9. Schematic diagram of the photon losses on mode  $a$ . The losses occurs after the  $U_\phi$ .

The QFI with photon losses is calculated as detailed in Ref. [67]. After the first OPA  $U_{S_1}$ , the Gaussian operation  $S_a$ , the phase shift  $U_\phi$ , the photon losses  $U_B$ , and before the detection, the output state in an expanded space can be given by

$$|\Psi_S\rangle = U_B U_\phi S_a |0\rangle_{a_v} |\psi\rangle, \quad (10)$$

a form of pure state, where  $|\psi\rangle = U_{S_1} |\alpha\rangle_a |0\rangle_b$ .

For the case of photon losses, we can treat the system as a pure state in an extended space, similar to Eq. (3). Then following Eq. (6), we can obtain the QFI under the pure state, denoted as  $C_Q$ , which is larger or equal to the QFI for mixed state, denoted as  $F_L$ , i.e.,  $F_L \leq$



$C_Q$ .  $C_Q$  is the QFI before optimizing over all possible measurements, i.e.,

$$C_Q = 4 \left[ \langle \psi | H_1 | \psi \rangle - |\langle \psi | H_2 | \psi \rangle|^2 \right], \quad (11)$$

where  $H_1$  and  $H_2$  are defined as

$$H_1 = \sum_{l=0}^{\infty} \frac{d}{d\phi} \Pi_l^\dagger(\eta, \phi, \lambda) \frac{d}{d\phi} \Pi_l(\eta, \phi, \lambda), \quad (12)$$

$$H_2 = i \sum_{l=0}^{\infty} \left[ \frac{d}{d\phi} \Pi_l^\dagger(\eta, \phi, \lambda) \right] \Pi_l(\eta, \phi, \lambda). \quad (13)$$

Here,  $\Pi_l(\eta, \phi, \lambda) = \sqrt{\frac{(1-\eta)^l}{l!}} e^{i\phi(n-\lambda)} \eta^{\frac{n}{2}} a^l$  is the phase-dependent Krause operator, satisfying  $\sum \Pi_l^\dagger(\eta, \phi, \lambda) \Pi_l(\eta, \phi, \lambda) = 1$ , with  $\lambda = 0$  and  $\lambda = -1$  representing the photon losses before the phase shifter and after the phase shifter, respectively.  $n = a^\dagger a$  is the number operator, and  $\eta$  is related to the dissipation factor with  $\eta = 1$  and  $\eta = 0$  being the cases of complete lossless and absorption, respectively. Following the spirit of Ref. [67], we can further obtain the minimum value of  $C_Q$  by optimizing over  $\lambda$ , corresponding to  $F_L$ , i.e.,  $F_L = \min C_Q \leq C_Q$ . Simplifying the calculation process allows us to derive the QFI under photon losses:

$$F_L = \frac{4F\eta \langle n_a \rangle}{(1-\eta)F + 4\eta \langle n_a \rangle}, \quad (14)$$

where  $F$  is the QFI in the ideal case [27].

Next, we further analyze the effects of each parameter on the QFI of the single-path LSO scheme under photon losses by numerical calculation. Fig. 10 plots the QFI and QCRB as functions of transmittance  $\eta$ , from which it is observed that the QFI and the QCRB improve with the rising transmittance  $\eta$ , and the single-path LSO can enhance the QFI and the QCRB. The improved QFI increases with the transmittance  $\eta$ , while the improved  $\Delta\phi_{QCRBL}$  decreases with the transmittance  $\eta$ .

Similar to the ideal case, Fig. 11 illustrates the QFI as a function of  $g$  ( $\alpha$ ) for a given  $\alpha$  ( $g$ ), under photon-loss case with  $\eta = 0.5$ . Similar to Fig. 7, The improvement in QFI increases with increasing values of the squeezing parameter  $r$  and  $g$  ( $\alpha$ ).

## V. CONCLUSION

In this paper, we have analyzed the effects of the single-path LSO scheme on the phase sensitivity and the QFI in both ideal and photon-loss cases. Additionally, we have investigated the effects of the squeezing parameter  $r$  of the single-path LSO scheme, the gain coefficient  $g$  of the OPAs, the amplitude  $\alpha$  of the coherent state and the transmittance  $T_k$  of the BSs on the performance of the system. Through analytical comparison, we have verified that the single-path LSO scheme can improve the measurement accuracy of the SU(1,1) interferometer

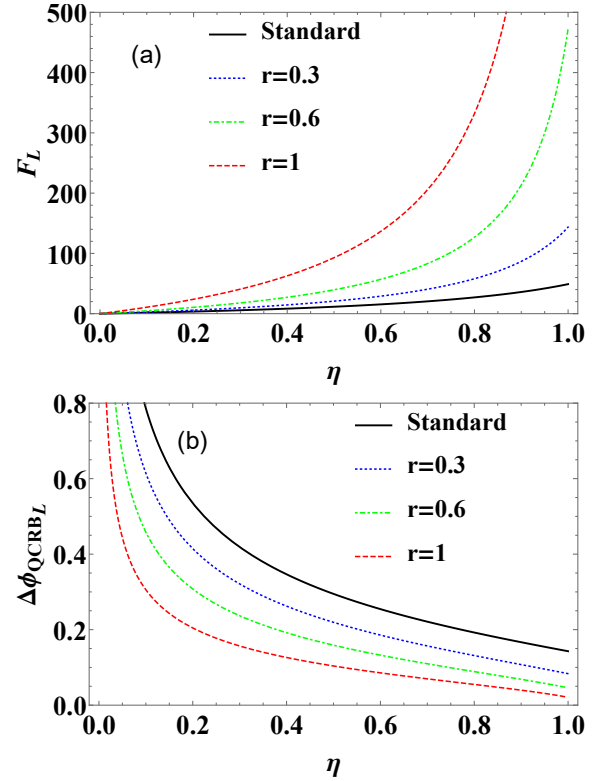


FIG. 10. The  $F_L$  and  $\Delta\phi_{QCRBL}$  as functions of transmittance  $\eta$ , with  $g = 1$  and  $\alpha = 1$ .

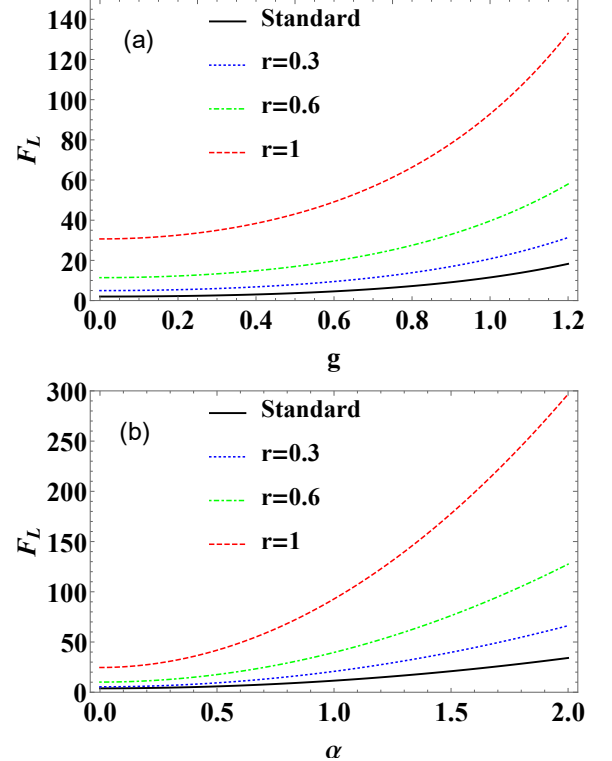


FIG. 11. (a) The  $F_L$  as a function of  $g$ , with  $\alpha = 1$  and  $\eta = 0.5$ . (b) The  $F_L$  as a function of  $\alpha$ , with  $g = 1$  and  $\eta = 0.5$ .

and enhance the robustness against internal and external photon losses. Throughout the entire range of  $T_k$ , internal losses have a more significant impact on the system's phase sensitivity than external losses. This finding indicates that reducing internal photon losses can be crucial for improving overall performance when optimizing the design of a quantum interferometer.

Gaussian operations are extensively utilized in quantum optics and information processing due to their ease of implementation and high energy efficiency. They enable effective manipulation of quantum states with relatively straightforward experimental setups, making them suitable for a wide range of applications. In contrast, non-Gaussian operations, while capable of generating a rich variety of quantum resources, present significant challenges. They are typically more complex to implement, often requiring sophisticated experimental techniques and precise control over system parameters. Additionally, these operations tend to be more energy-intensive, which can limit their practicality in certain scenarios. Our study highlights the potential of Gaussian operations to enhance the performance of quantum measurement and information processing systems.

In summary, the single-path LSO scheme is crucial in mitigating both internal and external photon losses in the SU(1,1) interferometer, thereby effectively improving the accuracy of quantum measurements. The Gaussian operation not only improves measurement reliability but also offers new insights and methods for future quantum technology applications.

#### ACKNOWLEDGMENTS

This work is supported by the National Natural Science Foundation of China (Grants No. 11964013 and No. 12104195) and the Jiangxi Provincial Natural Science Foundation (Grants No. 20242BAB26009 and 20232BAB211033), Jiangxi Provincial Key Laboratory of Advanced Electronic Materials and Devices (Grant No. 2024SSY03011), as well as Jiangxi Civil-Military Integration Research Institute (Grant No. 2024JXRH0Y07).

#### APPENDIX A : THE PHASE SENSITIVITY WITH THE SINGLE-PATH LSO SCHEME

In this appendix, we give the calculation formulas of the phase sensitivity with single-path LSO as follows:

$$\Delta\phi = \frac{\sqrt{\langle \Psi_{out}^1 | (a^\dagger + a)^2 | \Psi_{out}^1 \rangle - \langle \Psi_{out}^1 | (a^\dagger + a) | \Psi_{out}^1 \rangle^2}}{|\partial \langle \Psi_{out}^1 | (a^\dagger + a) | \Psi_{out}^1 \rangle / \partial \phi|}. \quad (A1)$$

Here, the output state  $|\Psi_{out}^1\rangle$  is given by Eq. (3), so the expectations related to the phase sensitivity in the single-path LSO scheme are specifically calculated as follows [39]:

$$\begin{aligned} & \langle \Psi_{out}^1 | (a^\dagger + a) | \Psi_{out}^1 \rangle \\ &= \langle \psi_{in} | U_{S_1}^\dagger S_a^\dagger [U_\phi^\dagger U_{B_1}^\dagger U_{S_2}^\dagger U_{B_2}^\dagger (a^\dagger + a) \\ & \times U_{B_2} U_{S_2} U_{B_1} U_\phi] S_a U_{S_1} | \psi_{in} \rangle \\ &= \sqrt{T_1 T_2} (e^{i\phi} Q_{1,0,0,0} + e^{-i\phi} Q_{0,1,0,0}) \cosh g \\ & + \sqrt{T_2} (Q_{0,0,0,1} + Q_{0,0,1,0}) \sinh g, \end{aligned} \quad (A2)$$

and

$$\begin{aligned} & \langle \Psi_{out}^1 | (a^\dagger + a)^2 | \Psi_{out}^1 \rangle \\ &= \langle \psi_{in} | U_{S_1}^\dagger S_a^\dagger [U_\phi^\dagger U_{B_1}^\dagger U_{S_2}^\dagger U_{B_2}^\dagger (a^\dagger + a)^2 \\ & \times U_{B_2} U_{S_2} U_{B_1} U_\phi] S_a U_{S_1} | \psi_{in} \rangle \\ &= T_1 T_2 (2Q_{1,1,0,0} + e^{2i\phi} Q_{2,0,0,0} + e^{-2i\phi} Q_{0,2,0,0}) \cosh^2 g \\ & + T_2 (2Q_{0,0,1,1} + 2 + Q_{0,0,2,0} + Q_{0,0,0,2}) \sinh^2 g \\ & + 2T_2 \sqrt{T_1} e^{i\phi} (Q_{1,0,0,1} + Q_{1,0,1,0}) \sinh g \cosh g \\ & + 2T_2 \sqrt{T_1} e^{-i\phi} (Q_{0,1,1,0} + Q_{0,1,0,1}) \sinh g \cosh g + 1, \end{aligned} \quad (A3)$$

where

$$\begin{aligned} & Q_{x_1, y_1, x_2, y_2} \\ &= \langle \psi_{in} | U_{S_1}^\dagger S_a^\dagger (a^{\dagger x_1} a^{y_1} b^{\dagger x_2} b^{y_2}) S_a U_{S_1} | \psi_{in} \rangle \\ &= \frac{\partial^{x_1 + y_1 + x_2 + y_2}}{\partial \lambda_1^{x_1} \partial \lambda_2^{y_1} \partial \lambda_3^{x_2} \partial \lambda_4^{y_2}} \{e^{w_4}\} |_{\lambda_1 = \lambda_2 = \lambda_3 = \lambda_4 = 0}, \end{aligned} \quad (A4)$$

with

$$\begin{aligned} w_1 &= \frac{1}{2} (\lambda_1^2 + \lambda_2^2) \cosh r \sinh r + \lambda_1 \lambda_2 \sinh^2 r \\ & - (\lambda_1 \cosh r \sinh g + \lambda_2 \sinh r \sinh g) \\ & \times (\lambda_3 \cosh g - \lambda_2 \cosh r \sinh g \\ & - \lambda_1 \sinh r \sinh g) \\ & - \lambda_4 \sinh g (\lambda_2 \cosh r \cosh g \\ & + \lambda_1 \sinh r \cosh g - \lambda_3 \sinh g), \end{aligned} \quad (A5)$$

$$w_2 = \lambda_1 \cosh r \cosh g + \lambda_2 \sinh r \cosh g - \lambda_4 \sinh g, \quad (A6)$$

$$w_3 = \lambda_2 \cosh r \cosh g + \lambda_1 \sinh r \cosh g - \lambda_3 \sinh g, \quad (A7)$$

$$w_4 = w_1 + w_2 \alpha^* + w_3 \alpha. \quad (A8)$$

[1] J. J. Cooper, D. W. Hallwood, and J. A. Dunningham, Entanglement-enhanced atomic gyroscope, Phys. Rev. A

81(4), 043624 (2010).

[2] W. Wasilewski, K. Jensen, H. Krauter, J. J. Renema,



- M. V. Balabas, and E. S. Polzik, Quantum Noise Limited and Entanglement-Assisted Magnetometry, *Phys. Rev. Lett.* 104(13), 133601 (2010).
- [3] F. Dolde, H. Fedder, M. Doherty, et al., Electric-field sensing using single diamond spins, *Nature Phys.* 7(6), 459 (2011).
- [4] H. Muntinga, et al., Interferometry with Bose-Einstein Condensates in Microgravity, *Phys. Rev. Lett.* 110(9), 093602 (2013).
- [5] C. F. Ockeloen, R. Schmied, M. F. Riedel, and P. Treutlein, Quantum Metrology with a Scanning Probe Atom Interferometer, *Phys. Rev. Lett.* 111(14), 143001 (2013).
- [6] K. Liu, C. X. Cai, J. Li, L. Ma, H. X. Sun, and J. R. Gao, Squeezing-enhanced rotating-angle measurement beyond the quantum limit, *Appl. Phys. Lett.* 113(26), 261103 (2018).
- [7] Y. Wu, J. X. Guo, X. T. Feng, L. Q. Chen, C. H. Yuan, and W. P. Zhang, Atom-Light Hybrid Quantum Gyroscope, *Phys. Rev. Applied* 14(6), 064023 (2020).
- [8] S. Y. Chen, W. H. Li, et al., Immunomagnetic microscopy of tumor tissues using sensors in diamond, *Proc Natl Acad Sci U S A* 119(5), e2118876119 (2022).
- [9] Q. Shen, J. Y. Guan, J. G. Ren, et al., Free-space dissemination of time and frequency with 10-19 instability over 113 km, *Nature* 610, 661 (2022).
- [10] C. M. Caves, Quantum-mechanical noise in an interferometer, *Phys. Rev. D* 23, 1693 (1981).
- [11] V. Giovannetti, S. Lloyd, and L. Maccone, Quantum-enhanced measurements: Beating the standard quantum limit, *Science* 306(5700), 1330 (2004).
- [12] V. Giovannetti, S. Lloyd, and L. Maccone, Advances in quantum metrology, *Nat. Photonics* 5(4), 222 (2011).
- [13] J. P. Dowling, Quantum optical metrology - the lowdown on high-NOON states, *Contemp. Phys.* 49(2), 125 (2008).
- [14] R. A. Campos, C. C. Gerry, and A. Benmoussa, Optical interferometry at the Heisenberg limit with twin Fock states and parity measurements, *Phys. Rev. A* 68, 023810 (2003).
- [15] P. M. Anisimov, G. M. Raterman, A. Chiruvelli, W. N. Plick, S. D. Huver, H. Lee, and J. P. Dowling, Quantum Metrology with Two-Mode Squeezed Vacuum: Parity Detection Beats the Heisenberg Limit, *Phys. Rev. Lett.* 104, 103602 (2010).
- [16] J. Liu, T. Shao, Y. X. Wang, M. M. Zhang, Y. Y. Hu, D. X. Chen, and D. Wei, Enhancement of the phase sensitivity with two-mode squeezed coherent state based on a Mach-Zehnder interferometer, *Opt. Express* 31, 27735 (2023).
- [17] Z. K. Zhao, Q. Q. Kang, H. Zhang, T. Zhao, C. J. Liu, and L. Y. Hu, Phase estimation via coherent and photon-catalyzed squeezed vacuum states, *Opt. Express* 32, 28267 (2024).
- [18] T. Nagata, R. Okamoto, J. L. O'Brien, K. Sasaki, and S. Takeuchi, Beating the standard quantum limit with four-entangled photons, *Science*, 316, 726 (2007).
- [19] B. Yurke, S. L. McCall, and J. R. Klauder, SU(2) and SU(1,1) interferometers, *Phys. Rev. A* 33(6), 4033 (1986).
- [20] J. Kong, F. Hudelist, Z. Y. Ou, and W. Zhang, Cancellation of internal quantum noise of an amplifier by quantum correlation, *Phys. Rev. Lett.* 111(3), 033608 (2013).
- [21] J. Jing, C. Liu, Z. Zhou, Z. Y. Ou, and W. Zhang, Realization of a nonlinear interferometer with parametric amplifiers, *Appl. Phys. Lett.* 99(1), 011110 (2011).
- [22] F. Hudelist, J. Kong, C. J. Liu, J. T. Jing, Z. Y. Ou, and W. P. Zhang, Quantum metrology with parametric amplifier-based photon correlation interferometers, *Nat. Commun.* 5(1), 3049 (2014).
- [23] M. V. Chekhova and Z. Y. Ou, Nonlinear interferometers in quantum optics, *Adv. Opt. Photon.* 8, 104 (2016).
- [24] Z. Y. Ou and X. Li, Quantum su(1,1) interferometers: Basic principles and applications, *APL Photonics* 5(8), 080902 (2020).
- [25] C. M. Caves, Reframing SU(1,1) interferometry, *Adv. Quantum Technol.* 3(11), 1900138 (2020).
- [26] S. K. Chang, C. P. Wei, H. Zhang, Y. Xia, W. Ye, and L. Y. Hu, Enhanced phase sensitivity with a nonconventional interferometer and nonlinear phase shifter, *Phys. Lett. A* 384(29), 126755 (2020).
- [27] S. K. Chang, W. Ye, H. Zhang, L. Y. Hu, J. H. Huang, and S. Q. Liu, Improvement of phase sensitivity in an SU(1,1) interferometer via a phase shift induced by a Kerr medium, *Phys. Rev. A* 105(3), 033704 (2022).
- [28] J. Kong, Z. Y. Ou, and W. Zhang, Phase-measurement sensitivity beyond the standard quantum limit in an interferometer consisting of a parametric amplifier and a beam splitter, *Phys. Rev. A* 87(2), 023825 (2013).
- [29] S. S. Szigeti, R. J. Lewis-Swan, and S. A. Haine, Pumped-up SU(1, 1) interferometry, *Phys. Rev. Lett.* 118(15), 150401 (2017).
- [30] G. Frascella, E. E. Mikhailov, N. Takanashi, R. V. Zakharov, O. V. Tikhonova, and M. V. Chekhova, Wide-field SU(1,1) interferometer, *Optica* 6(9), 1233 (2019).
- [31] W. Du, J. F. Chen, Z. Y. Ou, and W. Zhang, Quantum dense metrology by an SU(2)-in-SU(1,1) nested interferometer, *Appl. Phys. Lett.* 117(2), 024003 (2020).
- [32] D. Liao, J. Xin, and J. Jing, Nonlinear interferometer based on two-port feedback nondegenerate optical parametric amplification, *Opt. Commun.* 496, 127137 (2021).
- [33] J. D. Zhang, C. You, C. Li, and S. Wang, Phase sensitivity approaching the quantum Cramér-Rao bound in a modified SU(1,1) interferometer, *Phys. Rev. A* 103, 032617 (2021).
- [34] H. Ma and Y. Liu, Super-resolution localization microscopy: Toward high throughput, high quality, and low cost, *APL Photonics* 5(6), 080902 (2020).
- [35] Y. K. Xu, S. K. Chang, C. J. Liu, L. Y. Hu, and S. Q. Liu, Phase estimation of an SU(1,1) interferometer with a coherent superposition squeezed vacuum in a realistic case, *Opt. Express* 30, 38178 (2022).
- [36] A. M. Marino, N. V. Corzo Trejo, and P. D. Lett, Effect of losses on the performance of an SU(1,1) interferometer, *Phys. Rev. A* 86(2), 023844 (2012).
- [37] Z. Y. Ou, Enhancement of the phase-measurement sensitivity beyond the standard quantum limit by a nonlinear interferometer, *Phys. Rev. A* 85(2), 023815 (2012).
- [38] L. Y. Hu, M. Al-amri, Z. Y. Liao, and M. S. Zubairy, Entanglement improvement via a quantum scissor in a realistic environment, *Phys. Rev. A* 100, 052322 (2019).
- [39] Q. Q. Kang, Z. K. Zhao, T. Zhao, C. J. Liu, and L. Y. Hu, Phase estimation via a number-conserving operation inside a SU(1,1) interferometer, *Phys. Rev. A* 110(2), 022432 (2024).
- [40] H. Zhang, W. Ye, C. P. Wei, C. J. Liu, Z. Y. Liao, and L. Y. Hu, Improving phase estimation using number-conserving operations, *Phys. Rev. A* 103, 052602 (2021).
- [41] Q. Q. Kang, Z. K. Zhao, T. Zhao, C. J. Liu, and L. Y. Hu, Phase estimation via multi-photon subtraction inside the SU(1,1) interferometer, *Phys. Scr.* 99, 085111 (2024).

- [42] N. Namekata, Y. Takahashi, G. Fujii, D. Fukuda, S. Kurimura, and S. Inoue, Non-Gaussian operation based on photon subtraction using a photon-number-resolving detector at a telecommunications wavelength, *Nat. Photon.* 4, 655 (2010).
- [43] A. Zavatta, V. Parigi, and M. Bellini, Experimental non-classicality of single-photon-added thermal lightstates. *Phys. Rev. A* 75, 052106 (2007).
- [44] V. Parigi, A. Zavatta, M. Kim, and M. Bellini, Probing quantum commutation rules by addition and subtraction of single photons to/from a light field, *Science* 317, 1890 (2007).
- [45] W. Ye, H. Zhong, Q. Liao, D. Huang, L. Y. Hu, and Y. Guo, Improvement of self-referenced continuous variable quantum key distribution with quantum photon catalysis, *Opt. Express* 27, 17186 (2019).
- [46] J. Sahota and D. F. V. James, Quantum-enhanced phase estimation with an amplified Bell state, *Phys. Rev. A* 88(6), 063820 (2013).
- [47] V. C. Usenko and F. Grosshans, Unidimensional continuous-variable quantum key distribution, *Phys. Rev. A* 92(6), 062337 (2015).
- [48] S. L. Zhang and P. V. Loock, Local Gaussian operations can enhance continuous-variable entanglement distillation, *Phys. Rev. A* 84(6), 062309 (2011).
- [49] J. Fiurasek, Improving entanglement concentration of Gaussian states by local displacements, *Phys. Rev. A* 84(1), 012335 (2011).
- [50] W. Ye, C. P. Chen, S. K. Chang, et al., Quantum-improved phase estimation with a displacement-assisted SU(1,1) interferometer, *Opt. Express* 31(25), 41850 (2023).
- [51] T. P. Purdy, P. -L. Yu, R. W. Peterson, N. S. Kampel, and C. A. Regal, Strong Optomechanical Squeezing of Light, *Phys. Rev. X* 3, 031012 (2013).
- [52] T. Ono, J. Sabines-Chesterking, H. Cable, J. L. O'Brien, and J. C. F. Matthews, Optical implementation of spin squeezing, *New J. Phys.* 19, 053005 (2017).
- [53] X. J. Zuo, Z. H. Yan, Y. N. Feng, J. X. Ma, X. J. Jia, C. D. Xie, and K. C. Peng, Quantum Interferometer Combining Squeezing and Parametric Amplification, *Phys. Rev. Lett.* 124(17), 173602 (2020).
- [54] N. Kalinin, T. Dirmeier, A. A. Sorokin, E. A. Anashkina, L. L. Sánchez-Soto, J. F. Corney, G. Leuchs, and A. V. Andrianov, Quantum-enhanced interferometer using Kerr squeezing, *Nanophotonics* 12(14), 2945-2952 (2023).
- [55] Y. K. Xu, T. Zhao, Q. Q. Kang, C. J. Liu, L. Y. Hu, and S. Q. Liu, Phase sensitivity of an SU(1,1) interferometer in photon-loss via photon operations, *Opt. Express* 31(5), 8414 (2023).
- [56] M. Xiao, L. A. Wu, and H. J. Kimble, Precision measurement beyond the shot-noise limit, *Phys. Rev. Lett.* 59(3), 278 (1987).
- [57] R. Demkowicz-Dobrzański, M. Jarzyna, and J. Kołodyński, Quantum Limits in Optical Interferometry, *Prog. Optics* 60, 345 (2015).
- [58] M. Bradshaw, P. K. Lam, and S. M. Assad, Ultimate precision of joint quadrature parameter estimation with a Gaussian probe, *Phys. Rev. A* 97(1), 012106 (2018).
- [59] D. Li, C. H. Yuan, Z. Y. Ou, and W. Zhang, The phase sensitivity of an SU(1,1) interferometer with coherent and squeezed-vacuum light, *New J. Phys* 16(7), 073020 (2014).
- [60] X. Y. Hu, C. P. Wei, Y. F. Yu, and Z. M. Zhang, Enhanced phase sensitivity of an SU(1,1) interferometer with displaced squeezed vacuum light, *Front. Phys.* 11(3), 114203 (2016).
- [61] D. Li, B. T. Gard, Y. Gao, C. H. Yuan, W. Zhang, H. Lee, and J. P. Dowling, Phase sensitivity at the Heisenberg limit in an SU(1,1) interferometer via parity detection, *Phys. Rev. A* 94(6), 063840 (2016).
- [62] S. Ataman, A. Preda, and R. Ionicioiu, Phase sensitivity of a Mach-Zehnder interferometer with single-intensity and difference-intensity detection, *Phys. Rev. A* 98(4), 043856 (2018).
- [63] D. Li, C. H. Yuan, Y. Yao, W. Jiang, M. Li, and W. Zhang, Effects of loss on the phase sensitivity with parity detection in an SU(1,1) interferometer, *J. Opt. Soc. Am. B* 35(5), 309106 (2018).
- [64] A. Zavatta, S. Viciani, and M. Bellini, Quantum-to-classical transition with single-photon-added coherent states of light, *Science* 306(5696), 660 (2004).
- [65] Q. K. Gong, X. L. Hu, D. Li, C. H. Yuan, Z. Y. Ou, W. P. Zhang, Intramode-correlation-enhanced phase sensitivities in an SU(1,1) interferometer, *Phys. Rev. A* 96(3), 033809 (2017).
- [66] J. Beltran and A. Luis, Breaking the Heisenberg limit with inefficient detectors, *Phys. Rev. A* 72(4), 045801 (2005).
- [67] B. M. Escher, R. L. de Matos Filho, and L. Davidovich, General framework for estimating the ultimate precision limit in noisy quantum-enhanced metrology, *Nat. Phys.* 7(5), 406 (2011).
- [68] C. W. Helstrom, Quantum detection and estimation theory, *J. Stat. Phys.* 1(2), 231 (1969).
- [69] C. W. Helstrom, Minimum mean-squared error of estimates in quantum statistics, *Phys. Lett. A* 25(2), 101 (1967).